NOTES AND CORRESPONDENCE

On Mixing Processes in Continental Cumulus Clouds

BARRY A. GARDINER AND DAVID P. ROGERS

Desert Research Institute, Reno, NV 89506

24 September 1985 and 18 July 1986

ABSTRACT

Results are presented from the 1981 Convective Cloud Precipitation Experiment (CCOPE). Aircraft data are analyzed from different flight levels within a convective cloud using the θ_q–Q mixing diagram (Paluch). Points on this diagram are characterized by updrafts, downdrafts and the variation of the virtual potential temperature at the penetration level. New growth appears to have occurred on the upshear side of the cloud and mixed with all levels in the environment as it ascended. Maintenance of the cloud appears to depend on a balance between entrainment instability and dynamically forced airflow through cloud base. The results are discussed within the framework of a conceptual model for cloud evolution.

1. Introduction

Mixing processes within convective clouds have received considerable attention over the years. Essentially two basic interpretations of the process prevail. Stommel (1947) and Morton (1957) argued that entrainment in clouds is similar to that observed in plumes; whereas Scorer and Ludlam (1953) suggested that entrainment resembles that observed in laboratory "thermals." Clouds that behave like plumes entrain outside air through their sides and carry it along with the updraft. Warner (1970) investigated several plume models and showed that such models are incapable, with a single entrainment rate, of predicting observed values of liquid water content and cloud depth. He concluded that the simple idea of lateral entrainment is not sufficient when describing natural clouds. Turner (1973) pointed out that so-called starting plumes, which are a phenomenon related to both plumes and thermals, allow to some extent for mixing at the top as well as the sides, but concluded that a fully time-dependent approach is needed. In contrast, mixing in a thermal is confined to its top, and the mixed air is then carried down the sides and back into the bottom of the thermal.

Squires (1958) showed that cloud air mixed with environmental air may produce negatively buoyant mixtures. He noted that vertical mixing through the cloud top provides a better explanation for the observed liquid water content and lapse rate in small nonprecipitating cumuli than does entrainment based on either the plume or thermal model. Telford (1975) argued that mixing in clouds is primarily a buoyancy-driven process, and therefore, cloud air consisting of a series of parcels should be near buoyancy equilibrium (Telford et al., 1984).

It is the purpose of this note to discuss these processes based on a reinterpretation of the wet equivalent potential temperature mixing diagram. The data used were obtained during the Convective Cloud Precipitation Experiment (CCOPE 1981) by the University of Wyoming King Air and the Desert Research Institute Aerocommander aircraft. The discussion is based on a case study from 19 July 1981, which has been previously analyzed by several authors (Gardiner et al., 1985; Dye et al., 1986; Rogers et al., 1985).

2. The mixing diagram

In the absence of significant amounts of ice or precipitation sized particles, it is possible to determine the origin of entrained air in a cloud from conservative thermodynamic and microphysical quantities. This has been discussed in detail by Paluch (1979). Two parameters are defined; the total mixing ratio, Q, and the wet equivalent potential temperature, θ_q. The latter is a measure of the specific entropy and is conserved along the reversible adiabat.

Paluch found that, in general, a plot of θ_q against Q gave in-cloud points which lay on a straight line that intersected the environmental sounding at two points. One point represents the conditions of air flowing into cloud base, the other the origin of entrained air. This implies that mixing involves two discrete levels only, with mixing proportions varying along the line. A schematic representation of this mixing process is shown in Fig. 1. Several other authors (e.g., LaMontagne and Telford, 1983; Jensen et al., 1985) present additional evidence in support of this hypothesis. They observed that entrainment occurs predominantly

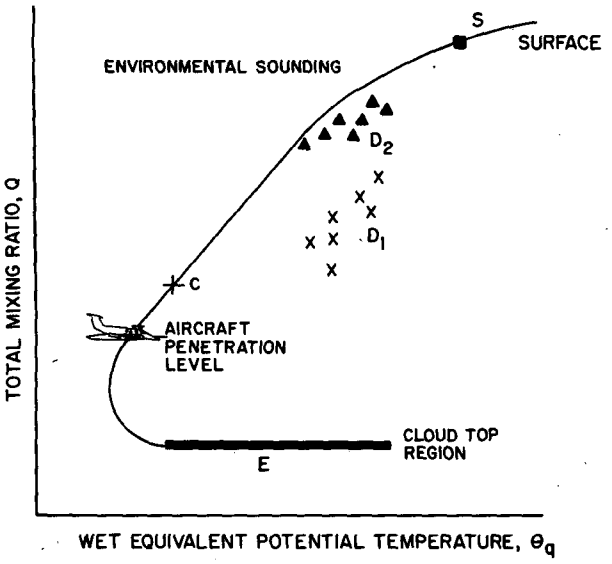

FIG. 1. Schematic representation of cloud mixing on a θ_q–Q diagram. Here S represents the source of cloud base air, C is the cloud base pressure level in the unmodified environment, E the source of entrained air, and D_1 are in-cloud data points representing a mixture of air from E and S. This indicates that mixing has occurred with air from above the flight level. D_2 represents air that is a mixture of S and the environment below the flight level.

at levels high above cloud base. Jensen et al. argued that in some cumuli there are only two thermodynamically well defined sources of cloud air—cloud base and cloud top. Telford and Wagner (1974) suggested that air motion measurements showed that there was no measurable flow in through the sides of the cloud which could be attributed to entrainment. In Paluch's (1979) observations the estimated entrainment levels were always below the level of cloud top at the time when the data were collected. She noted that there is some ambiguity in this observation, since it is not possible to deduce whether the air was entrained through cloud top at some earlier time or whether it was entrained through the sides of the cloud at some later time (Fankhauser et al., 1982). In addition, Paluch noted that in not all cases do the points follow orderly straight lines since there is no particular reason why all the entrained air should originate from the same altitude.

If the plume model were applicable, then the θ_q–Q points should lie close to the sounding curve, i.e., the air would have originated below the observation level (Fig. 1). In this case the mixture would have higher liquid water contents than the thermal model mixing at cloud top, assuming both mixtures contain the same proportion of cloud base air.

3. Conceptual model

Recently, Rogers et al. (1985) discussed observational evidence of the temporal evolution of the microphysics of cloud parcels from their formation on the upshear side of the cloud to their final evaporation on the downshear side of the cloud. It was found that in the alongshear direction the droplet concentration decreases from a maximum on the upshear side to a minimum on the downshear side of the cloud, whereas across-shear the droplet concentration remains nearly constant across the cloud.

This was explained by treating the cloud as a series of parcels. If new growth occurs on the upshear edge of the cloud, existing cloud parcels must move downshear relative to the cloud outline. These parcels will be older than the newly formed cloud air and may therefore have undergone more dilution due to mixing with environmental air. If each new parcel is independent of the surrounding parcels, then the degree of dilution of the parcel must depend on entrainment from above. However, some mixing with the surrounding parcels must be expected. Also, if the entrainment rate is nearly constant, the most dilute parcels must also be the oldest. Each parcel eventually becomes negatively buoyant and descends to its equilibrium level where it will have a tendency to remain. When sufficient dilution has taken place the whole cloud column will begin to subside and evaporate.

The conceptual model therefore predicts a spatial variability in the amount of entrainment. The further downshear one moves the lower the percentage of cloud base air in the mixture. Also, on the downshear side of the cloud, parcels that have undergone the most entrainment will be found at the lowest levels in the cloud.

4. Observations

The observations discussed here have been described in detail by Rogers et al. (1985), Gardiner et al. (1985) and Dye et al. (1986). Data from two aircraft, the Wyoming King Air, H2, and the Aerocommander, H14, are analyzed. An intercomparison between H2 and H14 was performed on 6 August 1981, and a case study is analyzed for 19 July 1981.

a. Intercomparison between H2 and H14 on 6 August 1981

The H14 Rosemount temperatures are used instead of the reverse flow temperatures because the latter have been found to be occasionally unreliable for this aircraft. Temperatures for H2 and H14 are corrected using data from tower fly-bys on 6 July and 5 August and from an aircraft wingtip to wingtip comparison on 18 July. The 5 August reverse flow temperature measurements for H2 show no systematic bias when compared with the tower Assman psychrometer. Comparison between H2 and the Wyoming Queen Air, H10, on 21 July show similar agreement once H10 values were corrected by an earlier tower flyby intercomparison on 6 July. Consequently, we have chosen the reverse flow thermometer of H2 as the standard without any cor-

rections applied. Relative to the H2 temperatures, the H14 Rosemount shows a systematic overestimate of temperature by about 0.6°C from comparisons on 18 and 21 July and 6 August. This correction is applied to all H14 temperatures. Choice of the Rosemount is, perhaps, unfortunate in view of the wetting problems associated with this instrument (Heymsfield et al., 1979). However, a comparison between the Rosemount and reverse flow thermometers on board H14 on 19 July agree reasonably well within cloud (Fig. 2). Note the noise spikes on the reverse flow temperature trace. The H14 liquid water contents are corrected for all data by multiplying measured Johnson–Williams (J–W) probe values by 0.75. This factor is based on in-trail cloud penetrations with four other aircraft during CCOPE and intercomparison of the J–W with a forward-scattering spectrometer probe (FSSP) and formvar replicator-derived liquid water contents (Gardiner and Hallett, 1985). H2 J–W liquid water contents are corrected by a factor of 1.6 for 6 August and 2.3 for 19 July. These factors are based on aircraft intercomparisons, ground spray tests and flights through adiabatic cloud regions as discussed by Jensen (1985). Mixing diagrams are presented in Fig. 3 for H2 and H14 from an in-trail cloud penetration. The H2 preceded H14 into the cloud. There is generally good agreement between the data for the two aircraft, with the trend in the two sets of points having approximately the same slope. Values for total water content are somewhat higher for H2 than for H14, and this variation is due to H2 encountering a region with higher liquid water contents. The vapor mixing ratio is assumed to be saturated and therefore dependent directly on temperature.

b. 19 July case study

Observations are presented that demonstrate the usefulness of the mixing diagram to investigate the temporal and spatial evolution of a cloud. Figure 4 shows the flight track for H2 plotted in a Lagrangian coordinate system with respect to the mean movement of the cloud. Cloud passes a and d are generally oriented along shear; passes b, c and e are essentially across wind and across shear. A time series for pass d is shown in Fig. 5. The precipitation amount, P_2, is measured by the two-dimensional precipitation probe (2-DP); C_2

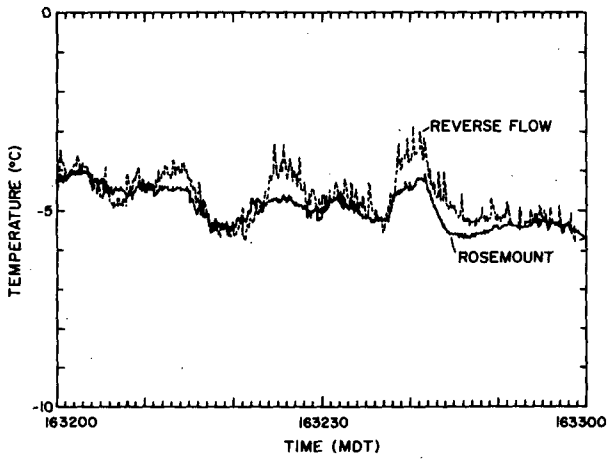

FIG. 2. Intercomparison between H14 reverse flow and Rosemount temperatures for an in-cloud penetration between 1632:00 and 1633:00 MDT 19 July 1981.

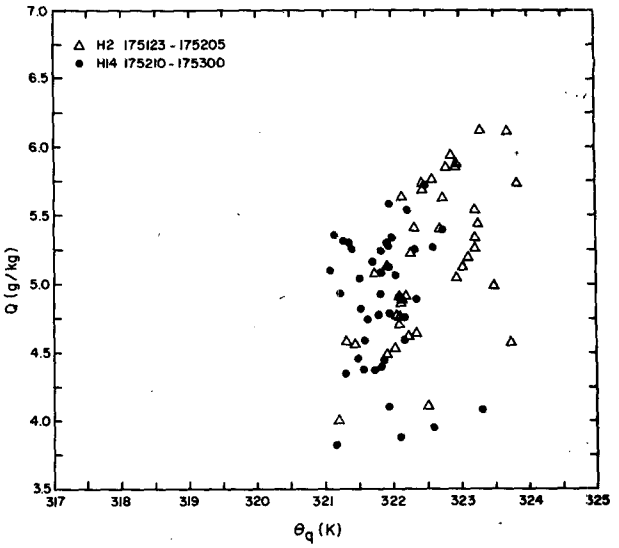

FIG. 3. Intercomparison between H14 and H2 on 6 August 1981. Data plotted on a θ_q–Q diagram.

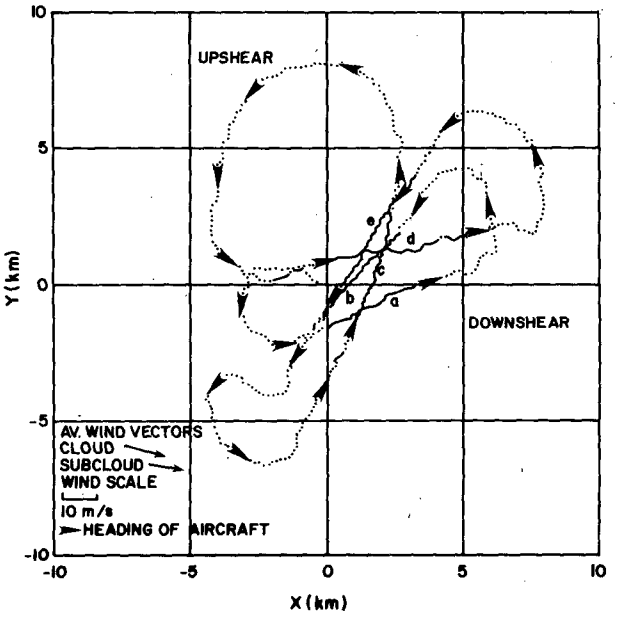

FIG. 4. Wyoming King Air flight path between 1618:25 and 1633:00 MDT 19 July 1981, plotted relative to the mean motion of the air. A mean wind speed of 15 m s^{-1} and direction of 270° is assumed within the cloud. Cloud penetrations are represented by solid lines. The coordinate system is centered on 1618:25 MDT.

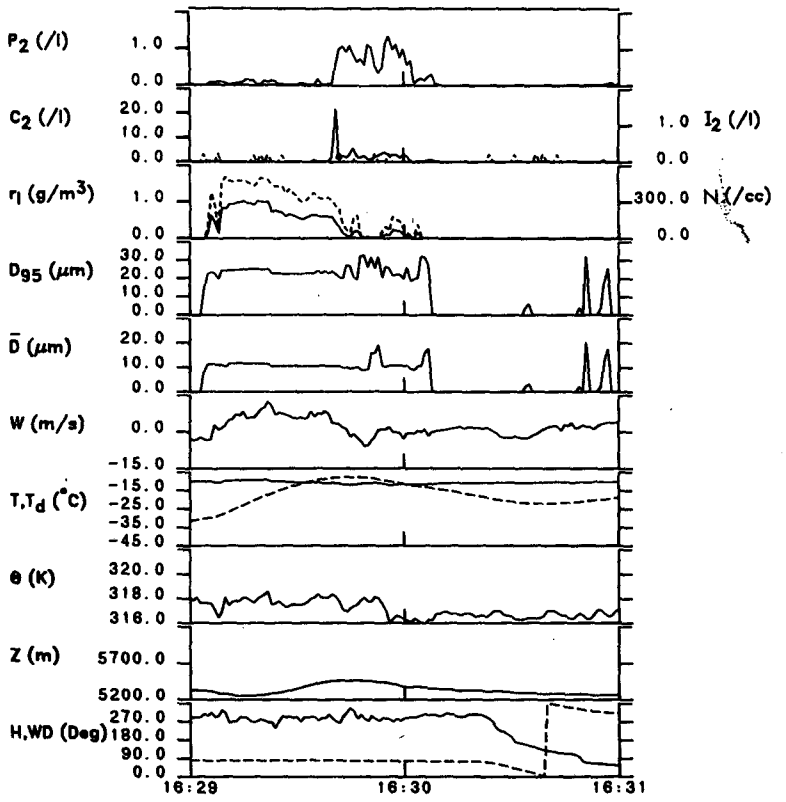

FIG. 5. Time series of pass d through a single cloud between 1629:00 and 1631:00 MDT 19 July 1981. See text for an explanation of symbols.

is the total concentration and I_2 is the polarized ice concentration (dashed line) measured by the two-dimensional cloud probe (2-DC); r_1 is the liquid water content and N is the droplet concentration (dashed line) in the nominal 2–32 μm diameter range measured by the FSSP; D_{95} is the 95% droplet volume diameter (diameter of the largest droplets); $\bar{D}$ is the mean diameter; and W is the vertical velocity. The T and T_d (dashed line) are temperature and dewpoint, respectively; θ is the potential temperature; Z the height above the ground; H (dashed line) the aircraft heading; and WD the wind direction. This time series was discussed by Rogers et al. (1985).

A θ_q–Q plot for the period 1629:00 to 1630:20 MDT (Mountain Daylight Time), corresponding with pass d, is shown in Fig. 6. These data are plotted as one second averages. The × and ○ identify the updrafts and downdrafts, respectively. The environmental sounding was derived from a radiosonde ascent at Miles City at 1100 MDT and the King Air climbout. Later soundings at Miles City at 1440 MDT and Knowlton at 1800 MDT showed little change in the environment. S indicates the condition of the air entering cloud base as determined by the NOAA/NCAR sailplane, H9, which passed through cloud base at 1619:28 MDT. The discrepancy between S and the environmental curve can be partly accounted for by errors in the temperature, pressure and mixing ratio as obtained from the radiosonde/aircraft and sailplane (see Fig. 6). Part of the discrepancy is probably due to differences in time and space between cloud and sounding. Typical errors for the aircraft derived in-cloud points are also shown in Fig. 6.

The observed minimum and maximum cloud top heights were at 450 and 250 mb, respectively. Figure 6 shows that the updrafts are predominantly associated with air that does not include air entrained at cloud top. Rather, dilution has occurred by mixing of air from close to and even below the aircraft penetration level. In contrast, air associated predominantly with downdrafts is diluted with air from above the penetration level but still below cloud top. The updraft region generally corresponds with the upshear side of the cloud.

Figure 7 shows a numbered sequence of θ_q–Q points for the same pass as Fig. 6. The aircraft entered the cloud at the upshear side. Each point represents a one second increment from 1629:00 MDT. Points that are outside the cloud are not plotted. These are points where either the liquid water content is less than 0.01 g m^{-3} or the FSSP strobe count is zero for more than 0.1 sec (the minimum response time of the J-W and temperature probes). Consideration has also been taken of the possible effects of glaciation. Estimates of the ice

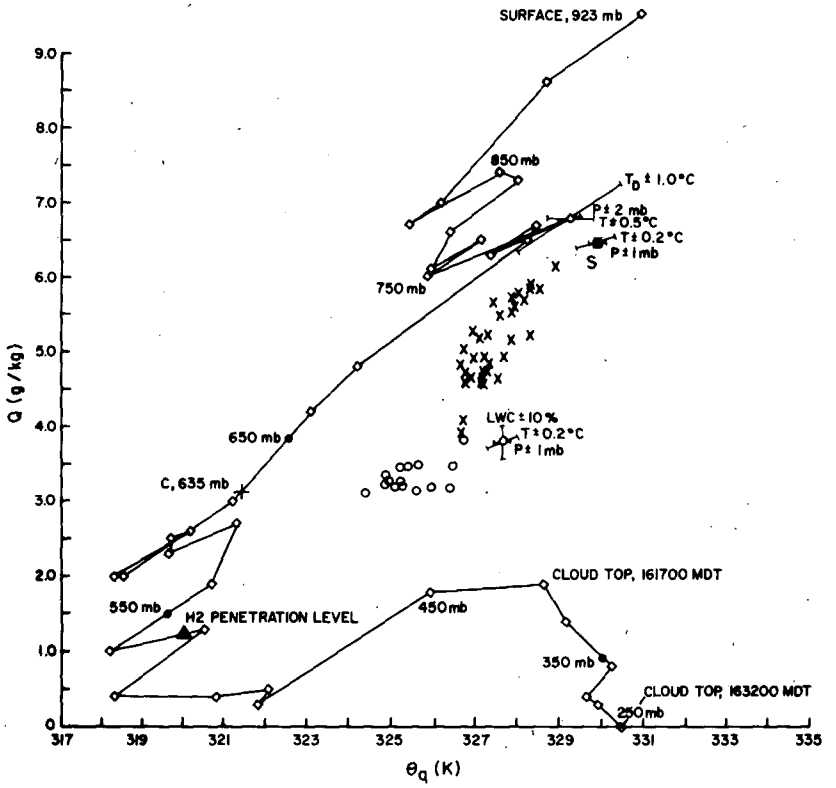

FIG. 6. θ_q–Q plot for H2 between 1629:00 and 1630:20 MDT 19 July 1981, corresponding with the pass shown in Fig. 5. Updrafts and downdrafts are represented by × and O, respectively. Selected pressure levels are shown on the environmental curve. S is determined from a sailplane ascent through cloud base at 1619:28 MDT. The effects of θ_q,Q values for typical errors in radiosonde and aircraft derived parameters are shown.

mass were obtained from the 2-DC and 2-DP probes. The highest ice mass detected in this pass was 0.3 g m^{-3}, but it was almost always less than 0.1 g m^{-3}. Those periods for which the ice mass was greater than 0.1 g m^{-3} are circled in Fig. 7, and the error introduced in the θ_q and Q values by an ice mass of 0.1 g m^{-3} is also shown. The effect of ice loading is obviously insignificant for ice masses less than 0.1 g m^{-3}. Even those points where the ice mass was greater than 0.1 g m^{-3} do not appear to have been significantly affected since points adjacent in time, where little ice was detected, have almost identical θ_q,Q values. Probably the ice had originated at higher elevations and the majority of its growth was due to depletion of liquid water above the observation level. This is supported by the radar data, which shows precipitation developing at 8 km and then falling through the cloud. Furthermore, the tendency of glaciation is to shift the measured characteristics toward higher θ_q values and toward lower Q values, and hence if the trend line for θ_q–Q measurements indicates a level of origin, that level is a reliable upper limit. Consistently high (>3 L^{-1}) ice concentrations were not encountered until about 1636 MDT.

The initial points in Fig. 7 correspond with a narrow downdraft region that was encountered at the edge of the cloud. This is observed in many growing clouds where the environmental air subsides to preserve continuity. Consequently, these points represent air that originated higher up in the environment. As the aircraft penetrates the main updraft, we note that, close to the upshear edge, the cloud air is the least dilute. This corresponds with the newest air in the cloud and must be closest to the core of the main updraft which is, essentially, undiluted. The scatter in the points suggests that air mixed in these updrafts is characteristic of entrainment from successive levels in the environment as the cloud layer grows upward, or alternatively, lateral entrainment through the side of the cloud may have occurred. In contrast, the region with maximum dilution between 1629:42 and 1629:52 MDT has mixed with air from the highest level observed during this penetration. This level is well above the penetration altitude but still below cloud top height at this time. Since this period corresponds with downdrafts, the implication is that this is cloud air that entrained environmental air at cloud top earlier in the life cycle of the cloud and is now descending.

Figure 8 is similar to Fig. 6 but indicates the virtual potential temperature perturbation (θ_v') within the cloud, where θ_v includes the liquid water loading and

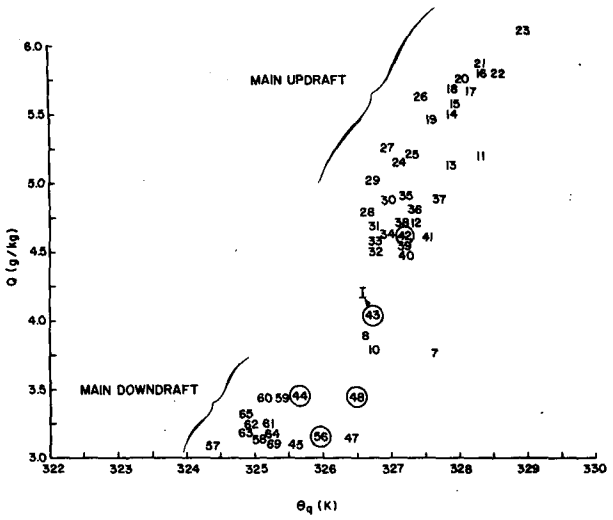

FIG. 7. A θ_q–Q plot for the same pass as Fig. 6, but showing a numbered sequence of points. Each point represents a one second increment from 1629:00 MDT. Only in-cloud points are plotted. The *I* indicates the correction to the θ_q,Q value of point 43 when account is taken of an ice mass of 0.1 g m^{-3}. Circled points have an ice mass between 0.1 and 0.3 g m^{-3}. All other points have ice masses less than 0.1 g m^{-3}.

○ and △ represent positive and negative perturbations, respectively. Most of the air in updrafts has a positive θ_v perturbation associated with the upward transport of air with a higher θ_v than the surrounding cloudy air (positively buoyant updrafts). Similarly, the downdrafts tend to bring down air that has a lower θ_v than the surrounding air (negatively buoyant downdrafts). This suggests that mixing of air down into the cloud from higher levels is due to entrainment instability, i.e., the local flux of θ_v within the cloud is positive. The points that lie close to the mean virtual potential temperature, $\bar{\theta}_v$, line are close to their buoyancy equilibrium level relative to the surrounding cloud environment, i.e., $\overline{w'\theta'_v} = 0$. Because the pressure level of the aircraft varied during the pass (510–522 mb), some of these points are just on the wrong side of the $\bar{\theta}_v$ line since a small error is introduced by not calculating the θ_v values from exactly the same pressure level.

The corresponding cloud pass in an alongshear direction for H14 was between 1631:45 and 1632:45 MDT. The H14 entered the cloud at the −4°C (595 mb) level. Radar data indicate that this pass was just south of the major updraft region. The liquid water content varied up to 0.35 g m^{-3} (70% of adiabatic),

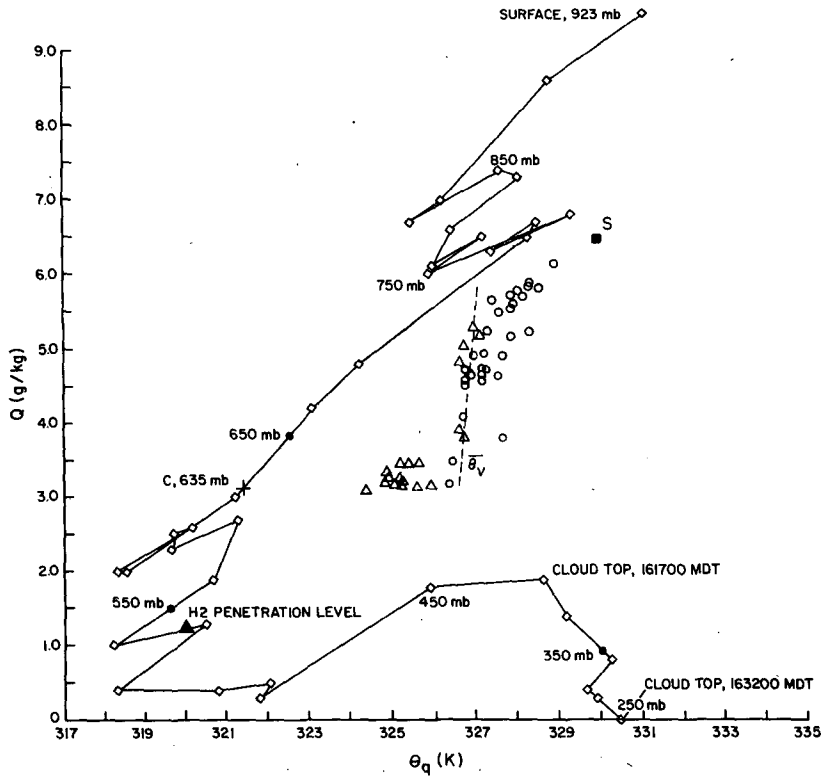

FIG. 8. As for Fig. 6, except positive and negative perturbations of virtual potential temperature (θ_v) are shown. The ○ and △ represent positive and negative perturbations, respectively. The mean virtual potential temperature for this pass, calculated for a pressure of 515.04 mb, is represented by a broken line.

with low LWC regions interspersed with regions of significant LWC (>0.2 g m^{-3}). Gardiner et al. (1985) noted that the narrow size distribution of droplets and relatively constant drop concentration indicate that the aircraft was flying through formative regions of the cloud. Somewhat lower drop concentrations were observed toward the downshear side of the cloud with maximum concentrations near the upshear edge. Ice was observed, but in negligible concentrations.

A θ_q–Q plot for this pass is shown in Fig. 9. In comparison with H2 (flying at 527 mb), most of the air encountered by H14 is a mixture of air from about the 550 mb level and lower. On average, the downdrafts (marked O) are mixtures of air from higher in the cloud than the corresponding updrafts (marked ×), which are presumably new growth. However, the difference between updrafts and downdrafts is less well defined than at the 527 mb level. It is possible that, at this stage in the cloud lifetime, organized parcels of air, originating higher up in the cloud, have not reached the H14 penetration level. Rather, the air seems to be a mixture of cloud base air and environmental air from well below the aircraft penetration level to approximately 550 mb.

Figure 10 shows a θ_q–Q plot for an acrosswind pass for H2 (marked b in Fig. 4) in which no ice was observed. These data are similar to those presented in Fig. 6 for an alongwind pass (marked d in Fig. 4). The similarity of the θ_q–Q plots for both passes supports the contention that the observed ice in pass d had a negligible influence on the validity of the θ_q–Q diagram (Fig. 6). In contrast with pass d, there is considerably less scatter in the data. This is consistent with the idea that cloud elements located acrosswind (perpendicular to the shear) should have a similar temporal history, (Rogers et al., 1985). Hence, those cloud parcels that are mixtures of environmental air must have entrained this air from a similar altitude (between 450 and 500 mb). In contrast, for pass d, entrainment has occurred between 450 and 700 mb. Furthermore, the data in Fig. 10 supports the sailplane-derived values of θ_q,Q for cloud base (point S).

5. Discussion

A number of recent papers (Boatman and Auer, 1983; LaMontagne and Telford, 1983; Jensen et al., 1985; Blyth and Latham, 1985) which have studied mixing processes within small continental cumulus clouds suggest that mixing occurs predominantly between two levels. Mixing occurs between a single level below cloud base that represents the air entering cloud

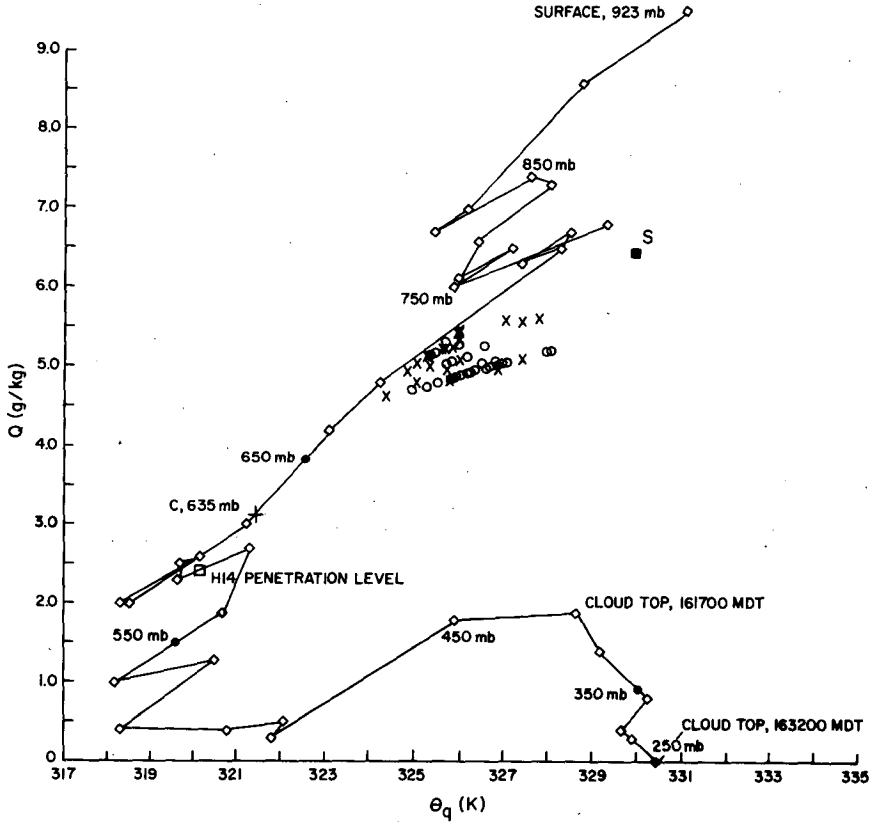

FIG. 9. As in Fig. 6 except for H14 between 1631:45 and 1632:45 MDT.

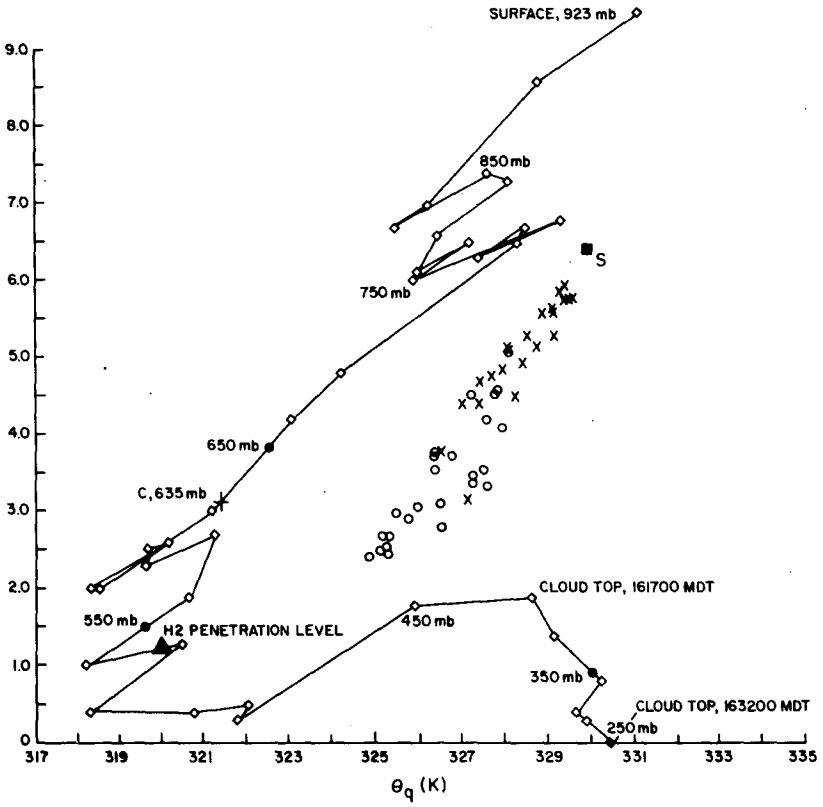

FIG. 10. As in Fig. 6 except for H2 between 1621:56 and 1622:47 MDT. (Acrosswind, across shear pass).

base and a point close to a quasi-stationary cloud top. This suggests that mixing within convective clouds is dynamically simple and is predominantly driven by evaporative cooling leading to penetrative downdrafts.

All of the aforementioned studies suffer from similar limitations. The clouds chosen tend to have a small vertical depth and are capped by very dry air through which the clouds cannot penetrate. This causes cloud top to stall and remain for a lengthy period of time close to one particular level. Under these conditions, entrainment from this quasi-stationary cloud top will be emphasized, and it becomes possible to approximate the mixing process to one occurring between two relatively well defined levels. However, this simple picture will not be universally applicable to convective clouds.

Furthermore, there is a tendency to emphasize the straightness of the lines on the θ_q–Q plots and ignore the fact that the spread in points provides additional information on the mixing process. As Paluch (1979) pointed out:

> Not all cloud Q, θ_q points fall along orderly straight lines which can be interpreted to be the result of mixing between two distinct levels of the sounding. The disorder is more pronounced when data from longer distances are plotted on the same graph. This is not surprising since there is no particular reason why all the entrained air should originate from the same altitude.

The purpose of this note is to show that the mixing type analysis, when combined with other measurements, provides a powerful tool for understanding the complex interaction between a cloud and its environment, both in the dynamic and microphysical sense. Interest in the 19 July case study was provoked when initial mixing type analyses for H14 and H2 gave very different suggestions as to the levels between which mixing was taking place. An in-trail penetration by H2 and H14 on 6 August showed there to be no systematic difference between the two aircraft which confirmed the validity of 19 July results. On 19 July, H14 flying at 595 mb found mixing to have occurred between 700 mb and all levels up to and around 550 mb (close to the aircraft penetration level and well below cloud top at the time). This, therefore, included mixing with air below cloud base as well as with environmental air between cloud base and 550 mb. A similar result was found during the National Hail Research Experiment by the Wyoming Queen Air flying close to cloud base (within 50–100 mb) and reported by Fankhauser et al. (1982). The Wyoming King Air (H2), on the other hand, flying between 527 and 516 mb observed mixing to be between 700 mb and points between 600 and 450 mb. Note that at the time of the first aircraft penetration of this cloud at 1617 MDT, cloud top was already at 430 mb and thereafter continued to rise to

its maximum height of 10.5 km (250 mb) by 1632 MDT. Therefore, the mixing observed by the aircraft in this cloud had to either

(i) have occurred prior to the first penetration,
(ii) occurred at cloud top during new growth of the cloud up to 450 mb, or
(iii) occurred due to lateral entrainment.

Environmental air from above 450 mb and hence mixing, which occurred at these higher levels during the rapid growth phase of the cloud (1621–1630 MDT), do not appear to have reached aircraft levels by 1633 MDT. Possibly, they reached these levels later, but after 1635 MDT, ice concentrations became too high for the mixing-diagram analysis to be valid.

By plotting different symbols on the θ_q–Q diagram for air with positive and negative perturbations of vertical velocity (Fig. 6), it is possible to see which air mixtures are moving upward relative to the average cloud motion and which are moving downward. Not surprisingly, the air that is moving downward appears to have undergone the most mixing and that moving upward has the greatest percentage of cloud base air. Furthermore, the downward-moving well-mixed air has entrainment sources above the level of aircraft penetration, whereas the upward-moving air has mixed predominantly with air at or even below the penetration level. The time series θ_q–Q plot (Fig. 7) provides additional information on the circulation in the cloud. The downshear decaying side of the cloud corresponds to the downward-moving air, the upshear edge with the growing least-mixed portion of the cloud. This confirms the earlier suggestion of Telford and Wagner (1974) that the upward-moving air is new growth on the upshear side of the cloud constantly mixing with the environment as it rises. The downward-moving air represents older growth that has previously reached its maximum altitude, where it had time to undergo considerable mixing with the environment, and is now descending and decaying downshear. Apart from the turret that underwent very vigorous growth between 1621 and 1630 MDT, most of the cloud appears to have reached a maximum altitude close to 450 mb, which corresponds to the very dry region between 500 and 400 mb seen in the 1440 MDT Miles City ascent (see Fig. 1 in Dye et al., 1986).

By plotting symbols for the positive and negative perturbations of virtual potential temperature rather than vertical velocity, something can also be learned of the buoyancy characteristics of the air mixtures (Fig. 8). This shows that negatively buoyant parcels are dominant in the older parts of the cloud. Although the entrainment rate associated with this process tends to be large (Deardorff, 1980), it is not clear whether entrainment can directly account for the dissipation of this cloud. Jensen et al. (1985) observed that small nonprecipitating clouds can have lifetimes of well over an hour even when vigorous entrainment of extremely dry air is taking place at cloud top. This supports the view that a cloud may be maintained by continued new growth on the upshear side of the cloud against the dissipating effect of entrainment instability. Consequently, some disruption of the airflow into the upshear side of the cloud, possibly by falling precipitation, may be responsible for the final decay of the cloud.

The evidence from this type of analysis lends support to the conceptual model introduced earlier and discussed in Rogers et al. (1985). New growth occurs on the upshear side of the cloud, with older, more dilute elements moving downshear. Mixing between cloud base air and the environment occurs at all levels up to the maximum height reached by the majority of the cloud. Although this may be due to lateral entrainment, it seems more likely that each new growing parcel mixes air from the surrounding environment as it moves upward. Cloud growth is restricted by dry air aloft, and the decaying cloud is carried downward by a combination of air moving to compensate for the new updrafts forming upshear and negative buoyancy following dry air entrainment. The evidence presented suggests that a balance is required between the dynamical forcing of the air flow directed into the cloud base, against the drying effect of entrainment. A possible reason for the cloud eventually dissipating is disruption of the flow into cloud base by falling precipitation, enabling entrainment of significant amounts of dry air to evaporate all of the cloud liquid water.

Evidence presented here suggests that the cloud dynamics and thermodynamics must be integrated to define the nature of the cloud microphysics. The interaction between cloud dynamics, microphysics, and the environment in which the cloud grows and which it eventually modifies, is an area of research that requires increased efforts if a true understanding of cloud evolution is sought.

Acknowledgments. Work reported here was supported under grants ATM-8020415, 8206558, 8209684 and 8419947, Meteorology Program, National Science Foundation, Washington, DC. We appreciate the help of James Telford, who pointed out an error in an earlier version of this paper. We would like to thank John Hallett, Ilga Paluch and Charles Knight for their many helpful comments and suggestions. Also, we would like to thank the Atmospheric Science Group of the University of Wyoming for access to the King Air data, and Katrina Lasko for drafting the figures.

REFERENCES

Blyth, A. M., and J. Latham, 1985: An airborne study of vertical structure and microphysical variability within a small cumulus. *Quart. J. Roy. Meteor. Soc.*, **111**, 773–792.

Boatman, J. F., and A. H. Auer, Jr., 1983: The role of cloud top entrainment in cumulus clouds. *J. Atmos. Sci.*, **40**, 1517–1534.

Deardorff, J. W., 1980: Cloud top entrainment instability. *J. Atmos. Sci.*, **37**, 131–147.

Dye, J. E., J. J. Jones, W. P. Winn, T. A. Cerni, B. Gardiner, D.

Lamb, R. L. Pitter, J. Hallett and C. P. R. Saunders, 1986: Early electrification and precipitation development in a small, isolated Montana cumulonimbus. *J. Geophys. Res.*, **91** (D1), 1231–1247.

Fankhauser, J. C., I. R. Paluch, W. A. Cooper, D. W. Breed and R. E. Rinehart, 1982: Air motion and thermodynamics. *Hailstorms of the Central High Plains,* Vol. I, NHRE, Colorado Associated University Press, 95–149.

Gardiner, B., D. Lamb, R. L. Pitter, J. Hallett and C. P. R. Saunders, 1985: Measurements of initial potential gradient and particle charges in a Montana summer thunderstorm. *J. Geophys. Res.*, **90**(D4), 6079–6086.

Gardiner, B. A., and J. Hallett, 1985: Degradation of in-cloud forward scattering spectrometer probe measurements in the presence of ice particles. *J. Atmos. Oceanic Technol.*, **2,** 171–180.

Heymsfield, A. J., J. E. Dye and C. J. Biter, 1979: Overestimates of entrainment from wetting of aircraft temperature sensors in cloud. *J. Appl. Meteor.*, **18,** 92–95.

Jensen, J. B., 1985: Turbulent mixing, droplet spectral evolution and dynamics of warm cumulus clouds. Ph.D. dissertation, University of Washington, 185 pp.

——, P. H. Austin, M. B. Baker and A. M. Blyth, 1985: Turbulent mixing, spectral evolution and dynamics in a warm cumulus cloud. *J. Atmos. Sci.*, **42,** 173–192.

LaMontagne, R. G., and J. W. Telford, 1983: Cloud top mixing in small cumuli. *J. Atmos. Sci.*, **40,** 2148–2156.

Morton, B. R., 1957: Buoyant plumes in a moist atmosphere. *J. Fluid Mech.*, **2,** 127–144.

Paluch, I. R., 1979: The entrainment mechanism in Colorado cumuli. *J. Atmos. Sci.*, **36,** 2467–2478.

Rogers, D. P., J. W. Telford and S. K. Chai, 1985: Entrainment and the temporal development of the microphysics of convective clouds. *J. Atmos. Sci.*, **42,** 1846–1858.

Scorer, R. S., and F. H. Ludlam, 1953: Bubble theory of penetrative convection. *Quart. J. Roy. Meteor. Soc.*, **79,** 94–103.

Squires, P., 1958: Penetrative downdrafts in cumuli. *Tellus,* **10,** 381–389.

Stommel, H., 1947: Entrainment of air into a cumulus cloud. *J. Meteor.*, **4,** 91–94.

Telford, J. W., 1975: Turbulence, entrainment and mixing in cloud dynamics. *Pure Appl. Geophys.*, **113,** 1067–1084.

——, and Wagner, P. B., 1974: The measurement of horizontal air motion near clouds from aircraft. *J. Atmos. Sci.*, **31,** 2066–2080.

——, T. S. Keck and S. K. Chai, 1984: Entrainment at cloudtops and the droplet spectra. *J. Atmos. Sci.*, **41,** 3170–3179.

Turner, J. S., 1973: Buoyancy effects in fluids. *Cambridge University Press,* 368 pp.

Warner, 1970: The microstructure of cumulus clouds. Part III: The nature of the updraft. *J. Atmos. Sci.*, **27,** 682–688.